

Title	Classification of processes for the atomic layer deposition of metals based on mechanistic information from density functional theory calculations
Authors	Elliott, Simon D.;Dey, Gangotri;Maimaiti, Yasheng
Publication date	2017-02-03
Original Citation	Elliott, S. D., Dey, G.; Maimaiti, Y. (2017) 'Classification of processes for the atomic layer deposition of metals based on mechanistic information from density functional theory calculations', Journal of Chemical Physics, 146(5), 052822 (11pp). doi:10.1063/1.4975085
Type of publication	Article (peer-reviewed)
Link to publisher's version	10.1063/1.4975085
Rights	© 2017, the Authors. Published by AIP Publishing. This article may be downloaded for personal use only. Any other use requires prior permission of the authors and AIP Publishing. The following article appeared in Elliott, S. D., Dey, G.; Maimaiti, Y., Journal of Chemical Physics, 146(5), 052822 (11pp), and may be found at http://dx.doi.org/10.1063/1.4975085
Download date	2024-07-24 18:57:21
Item downloaded from	https://hdl.handle.net/10468/5750



UCC

University College Cork, Ireland
Coláiste na hOllscoile Corcaigh

Supplementary Information for “Classification of processes for the atomic layer deposition of metals based on mechanistic information from density functional theory calculations”

S. D. Elliott,^{1,a)} G. Dey,^{2,b)} and Y. Maimaiti¹

¹*Tyndall National Institute, University College Cork, Lee Maltings, Dyke Parade, Cork, T12 R5CP, Ireland*

²*Rutgers University, Chemistry and Chemical Biology, Rutgers University, 174 Frelinghuysen Road, Piscataway, New Jersey, NJ 08854, USA*

S-I. METHOD FOR COMPUTING ADSORPTION OF Cu(acac)₂ (SECTION II OF MAIN PAPER)

The Vienna ab initio simulation package (VASP 5.3) was used for the periodic DFT calculations.¹ The projector augmented wave (PAW) approach² was applied for describing the effective potential of core electrons. The generalized gradient approximation (GGA) was employed with the correction for van der Waals forces in the vdW-optB88 functional.³ The wave functions were expanded in the plane wave basis up to a cutoff energy of 450 eV. Because of the large cell sizes, it was found to be adequate to use only the Γ point to sample the Brillouin zone for both slab and gas phase calculations. The atomic positions of ions were optimized using a conjugate gradient algorithm until the forces on each ion were smaller than 0.02 eV/Å. The geometry optimization for a single Cu(dmap)₂ molecule in the gas phase was performed by placing the molecule in a rhombohedral supercell with $\gamma = 60^\circ$ and a side length of 25 Å.

S-II. NON-INNOCENT DIAZADIENYL LIGAND (SECTION IV.C OF MAIN PAPER)

A. Computational method

The electronic structure of isolated complexes in the gas-phase was computed using spin-unrestricted Kohn-Sham density functional theory (DFT) with all electrons described by the atom-centered basis set⁴ def2-TZVPP, as implemented in the TURBOMOLE suite of programs.⁵ Unless otherwise stated, the results quoted here were obtained using the hybrid gradient-corrected functional⁶ PBE0. Tests were carried out on the Co(^tBu₂DAD)₂ complex using a variety of other DFT functionals and, as expected, it was observed that the partial inclusion of Hartree-Fock exchange in hybrid functionals had a substantial effect on spin-dependent properties. Dispersion-corrected functionals were not used, although there is mounting evidence that they can improve the description of weak ligand-ligand interactions.

Molecular geometries of M(^tBu₂DAD)₂ and M(Me₂DAD)₂ (M=Ti, V, Cr, Mn, Fe, Co, Ni, Cu) were optimized freely using redundant internal coordinates⁷ to obtain minimum energy structures for all possible spin configurations of each complex.

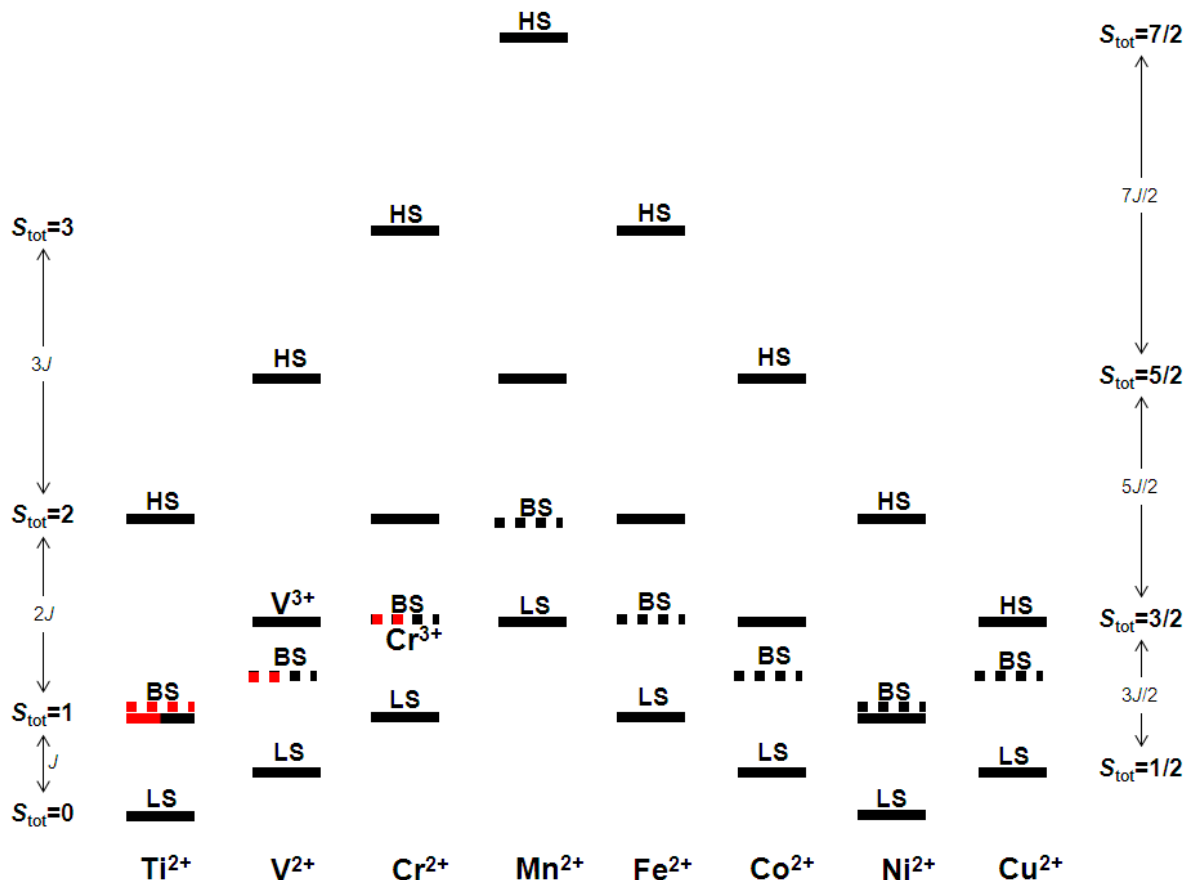


Figure 1: Ladder of energies of possible spin states for various $\text{M}(\text{BuDAD})_2$ complexes; HS=high total spin for the complex (ferromagnetic coupling), BS=broken symmetry, LS=low total spin (antiferromagnetic coupling). Red lines indicate that one or both ligands are ‘flattened’ due to M-N orbital overlap. The illustration is for $J < 0$, which means that low-spin states are energetically favored. The LS state is in general not accessible with single-determinant DFT but its energy can be estimated from $E_{\text{LS}} = E_{\text{BS}} + J$, where J for each system can be computed from E_{HS} , E_{BS} and the spin expectation values (Equation 1).

B. Approach for dealing with spin contamination

Substantial spin contamination (as monitored via the expectation value $\langle S^2 \rangle$) was a feature of most solutions, except the highest spin state. This error is typical when applying a single-reference approximation (such as Kohn-Sham DFT) to a multi-reference system (such as polynuclear transition metal complexes, organic biradicals or non-innocent ligands⁸).

We therefore apply the ‘broken symmetry’ (BS) approach,^{9, 10, 11} which assumes that the energy differences between spin configurations can be accounted for by a phenomenological spin Hamiltonian. Applying this formalism to our case (illustrated in Figure 1), the computed solutions for a spin-contaminated BS low-spin state and for an uncontaminated high

spin state for the whole complex (HS) can be used to estimate the energy of a spin-pure low-spin state of the complex (LS) via the Yamaguchi formula:¹²

Equation 1:

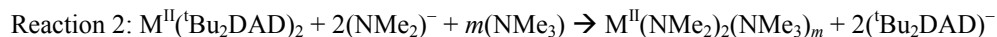
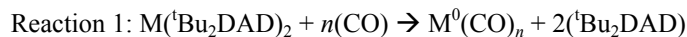
$$E_{LS} = E_{BS} + J$$

$$\text{where } J = [E_{HS} - E_{BS}] / [\langle S^2 \rangle_{HS} - \langle S^2 \rangle_{BS}].$$

The estimated energy of the low-spin state can then be used to evaluate the reactivity of the complex in that state. The coupling constants that we have obtained using this method with PBE0 range from $J=-4$ to $J=-19$ kJ/mol for the various metal complexes and so are chemically significant. Differences in J between ^tBu₂DAD and Me₂DAD seem to be insignificant. Tests on Co(^tBu₂DAD)₂ indicate slightly higher J for other hybrid functionals, and higher again for non-hybrid gradient-corrected functionals (up to double the PBE0 value).

Unfortunately, this approach does not allow explicit geometry optimization of the spin-pure low-spin state and so the structural parameters quoted here are those computed for the spin-contaminated BS geometry. Note that we fully optimize the geometries at each spin state and use the resulting total energies in Equation 1. This is not strictly in accordance with the BS formalism, but the error is small because the HS and BS geometries are so similar for most of the M(^tBuDAD)₂ complexes.

C. Approach for computing reaction energetics



Note that the charge of the co-reagent molecules (neutral in Reaction 1, negative in Reaction 2) must be reflected in the charge of the free DAD product. For each M, various values of n and m were tested in order to find the most stable product complex that has all ligands in the first coordination sphere (*e.g.* Cr(CO)₆ but Fe(CO)₅). Low-spin solutions were found to be lowest in energy for M(CO) _{n} , whereas high-spin solutions were favored for M(NR₂)₂(NR₃) _{m} . So as to focus on the changes in metal-ligand bonding, the energy differences for these reactions are quoted as $\Delta E(1)$ and $\Delta E(2)$ at $T=0$ K, with negative ΔE indicating energetically-favored forward reactions. Entropy is neglected and no activation energies are computed. There is no correction for zero-point energy or basis set superposition errors.

D. Results for each diazadienyl complex

Ti(DAD)₂: Coupling between triplet Ti(II):3d² ($S_M=1$) and triplet DAD⁻ ligands ($S_L=1$) can be ferromagnetic ($S_{\text{tot}}=2$), antiferromagnetic ($S_{\text{tot}}=0$), or in-between ($S_{\text{tot}}=1$), as shown in Figure 1. The lowest energy spin states computed with DFT are a low-spin BS state (a spin-contaminated singlet) and a medium-spin state (an uncontaminated triplet), with the latter just

1.5 kJ/mol lower in energy. Applying Equation 1 to either state yields roughly the same estimate of the energy of the spin-pure antiferromagnetic state; $J=-18.9$ kJ/mol. The geometries computed for medium-spin and low-spin BS are very similar. In each complex, the C-C distances would suggest that both ligands are monoanionic, but have slightly different charge distribution within the conjugated system. However, the two ligands are coordinated to Ti in different ways. One ligand is coordinated in the usual way, *i.e.* ‘end-on’ with co-planar Ti-N-C-C-N (Ti-C=288 pm, Ti-N=214 pm). The other ligand is ‘bent’, with the C-C segment of the ligand backbone angled sideways towards Ti, out of the N-Ti-N plane. This shortens the Ti-C distances to 233.1 pm, as well as shortening Ti-N to 194.1 pm and widening the N-Ti-N angle to just over 90°. This is indicative of back-bonding from occupied M:d orbitals into empty ligand π orbitals¹³ and thus of oxidation of the metal. Simplifying the situation considerably, we assign the oxidation state as Ti(III). Notwithstanding these differences, the ligating N atoms are disposed about Ti in a distorted tetrahedron in all spin states. This coordination environment is preserved when the bulk of the ligands is reduced to MeDAD. This demonstrates that there is no tendency towards Jahn-Teller distortion.

V(DAD)₂: Coupling between quartet V(II):3d³ ($S_M=3/2$) and triplet DAD⁻ ligands ($S_L=1$) can be ferromagnetic ($S_{tot}=5/2$) or antiferromagnetic ($S_{tot}=1/2$), as shown in Figure 1. Of all the possible spin states, a low-spin BS state is computed with DFT to be lowest in energy, but is substantially spin-contaminated. Using Equation 1 yields a spin-pure antiferromagnetic state that is 6 kJ/mol lower in energy. As with the low-spin Ti complex, one ‘bent’ ligand is a feature of the optimized geometry for the low-spin BS V complex. Here too, the C-C bond length of 138 pm indicates a monoanion, but the C-C segment of the ligand is tilted out of the N-V-N plane, giving shorter V-C (233.8 pm), shorter V-N (192 pm) and near-90° N-V-N angle. This is indicative of back-bonding from occupied M:d orbitals into empty ligand π orbitals¹³ and thus of oxidation of the metal. The other monoanionic ligand of this complex binds ‘end-on’ (V-C=281 pm, V-N=206 pm, N-V-N=81°). Simplifying the situation considerably, we assign the oxidation state as V(III). The spin-pure quartet state of V(^tBuDAD)₂ has an interesting structure. The ligands bind ‘end-on’ in an approximately tetrahedral fashion. However one ligand exhibits a C-C distance that is so short (135.1 pm) as to suggest a double bond, indicating that this ligand is a spin-free dianion, (^tBuDAD)²⁻, $S_L=0$. Short V-N distances support this. The C-C distance in the other ligand is consistent with the monoanion radical. Consequently, the formal oxidation state of the metal centre is V(III). The overall spin of this complex ($S_{tot}=3/2$) therefore results from ferromagnetic coupling between V(III):d² ($S_M=1$) and one DAD⁻ ligand ($S_L=1/2$). Approximately tetrahedral coordination of N atoms around V are also observed for the various spin states of the less sterically crowded complex V(MeDAD)₂. One ligand is flattened in both the low-spin BS and medium-spin cases. One ligand is a dianion in

the low-spin case, whereas both are monoanions in the medium-spin case, indicating that the fine details of electronic structure are sensitive to ligand bulk.

Cr(DAD)₂: Coupling between quintet Cr(II):3d⁴ ($S_M=2$) and triplet DAD⁻ ligands ($S_L=1$) can be ferromagnetic ($S_{tot}=3$), antiferromagnetic ($S_{tot}=1$) or in-between ($S_{tot}=2$) as shown in Figure 1. Of all the possible spin states, a low-spin BS state is computed with DFT to be lowest in energy, but only 3 kJ/mol more stable than the medium-spin BS state originating from one electron spin being flipped. Both of these BS states are substantially spin-contaminated and using either in Equation 1 yields roughly the same energy for a spin-pure antiferromagnetic state. The experimental structure¹⁴ of Cr(^tBuDAD)₂ combines the unusual features that we have observed in computed Ti and V complexes. One ligand is ‘bent’, with C-C tilting out of the N-Cr-N plane (Cr-C=235-236 pm), Cr-N shortening (192.4 pm) and the N-Cr-N angle opening to just over a right angle. The C-C bond length indicates that this flattened ligand is monoanionic. The other ligand of Cr(^tBuDAD)₂ binds ‘end-on’, co-planar with N-Cr-N, but is measured to have a short C-C bond (133.7 pm), consistent with dianionic charge. This accounts for the short distance between its N and Cr (193 pm). The geometry computed for medium-spin BS qualitatively reproduces these C-C and Cr-N distances. The metal centre is therefore formally Cr(III), although assigning a charge state is complicated by the partially-covalent bonding to the bent ligand. As with the V case, we note that both Cr(II) and Cr(III) are consistent with the measured magnetic moment. The geometry computed for the low-spin BS state has identical ligands, with C-C bonds that seem to be an average between monoanionic and dianionic cases. This illustrates the failings of approximate DFT in computing antiferromagnetic coupling in these cases. Cr-N distances are computed to become shorter with decreasing spin, consistent with more spin pairing in Cr-N bonding orbitals. (This finding is general to all the metal complexes considered here). The ligating N atoms are disposed about Cr in a distorted D_{2d} tetrahedron in Cr(^tBu₂DAD)₂ for all spin states. By contrast, Cr(Me₂DAD)₂ is nearly planar, again regardless of spin. This demonstrates that the distorted tetrahedron is electronically unstable with respect to Jahn-Teller distortion towards planar Cr(II), but that this can be prevented by bulky substituents on N. Consistent with this, replacement of ^tBu₂DAD ligands with Me₂DAD (and full relaxation) is computed to yield -46 to -61 kJ/mol depending on the spin state. This strain may account for a portion of the substantial energy that we predict would be released from Cr(^tBu₂DAD)₂ on ligand exchange to give an octahedral carbonyl complex, $\Delta E(1)$, or planar amine complex, $\Delta E(2)$.

Mn(DAD)₂: Mn(II):3d⁵ is the dication with the highest spin in the first row of transition metals. Coupling between this sextet ($S_M=5/2$) and triplet DAD⁻ ligands ($S_L=1$) can be ferromagnetic ($S_{tot}=7/2$) or antiferromagnetic ($S_{tot}=3/2$). A low-spin BS state is computed to be lowest in energy, in qualitative agreement with experiment, but is spin-contaminated and so is

used to estimate the energy of the spin-pure antiferromagnetic ground state of experiment (Equation 1). Geometries with ‘bent’ ligands were found to be unstable, optimizing to end-on configurations. Optimization of the Me_2DAD complex illustrates that there is no tendency towards Jahn-Teller distortion out of D_{2d} symmetry and a negligible difference in metal-ligand bond energy between $\text{Mn}(\text{Me}_2\text{DAD})_2$ and $\text{Mn}(\text{}^t\text{Bu}_2\text{DAD})_2$.

Fe(DAD)₂: Coupling between quintet $\text{Fe(II):}3d^6$ ($S_M=2$) and the triplet pair of DAD^- ligands ($S_L=1$) can be ferromagnetic ($S_{\text{tot}}=3$) or antiferromagnetic ($S_{\text{tot}}=1$), as already seen for Cr(II) . The lowest energy state computed with DFT is BS low-spin, in qualitative agreement with experiment, which allows us to estimate the energy of the spin-pure antiferromagnetic ground state. The computed C-C bond length of the low-spin BS state matches the X-ray structure¹⁴ to 0.2%, so that there can be little doubt about describing the ligands as monoanions and the metal as Fe(II) . However the Fe-N distance is computed to be 3% too long in the BS complex and 6% too long in the ferromagnetic complex, consistent with reduced occupancy of Fe-N bonding orbitals in the high-spin cases. Geometries with ‘bent’ ligands were found to be unstable, optimizing to end-on configurations. There is no tendency towards Jahn-Teller distortion out of D_{2d} symmetry in low-spin $\text{Fe}(\text{}^t\text{Bu}_2\text{DAD})_2$ or $\text{Fe}(\text{Me}_2\text{DAD})_2$ and so these complexes are almost equally stable.

Co(DAD)₂: Coupling between quartet $\text{Co(II):}3d^7$ ($S_M=3/2$) and triplet DAD^- ligands ($S_L=1$) can be ferromagnetic ($S_{\text{tot}}=5/2$) or antiferromagnetic ($S_{\text{tot}}=1/2$), as for the analogous vanadium complex. As with most of the other metals studied here, for Co the most stable structure in DFT is the lowest spin BS state, which suffers from substantial spin contamination. Applying Equation 1 yields an estimate for the energy of the spin-pure antiferromagnetic state obtained experimentally. Geometries with ‘bent’ ligands were found to be unstable, optimizing to end-on configurations. The experimental C-C bond lengths¹⁴ are reproduced almost exactly in the DFT calculations, but the Co-N distances are over-estimated, consistent with reduction of Co-N bonding character through spin contamination. There is no tendency towards Jahn-Teller distortion out of D_{2d} symmetry and so the Me_2DAD and $\text{}^t\text{Bu}_2\text{DAD}$ complexes are almost equally stable in terms of metal-ligand bonding.

Ni(DAD)₂: Coupling between triplet $\text{Ni(II):}3d^8$ ($S_M=1$) and triplet DAD^- ligands ($S_L=1$) can be ferromagnetic ($S_{\text{tot}}=2$) or antiferromagnetic ($S_{\text{tot}}=0$, *i.e.* diamagnetic), the same range of spin states as for Ti. For Ni, the lowest DFT energy is once again obtained for the spin-contaminated BS low-spin state (whereas a non-spin-polarised singlet state is nearly 100 kJ/mol higher in energy). The energy for the experimentally-observed antiferromagnetically coupled state is thus estimated via the BS formalism. As no geometry can be computed with DFT for the antiferromagnetic state, we compare that optimized for the low-spin BS state with the experimental geometry.¹⁴ The C-C bond length is underestimated by <1%. The Ni-N distance is overestimated by 3%. The N-Ni-N angle is underestimated by 1%. The ligating N atoms of the $\text{}^t\text{Bu}_2\text{DAD}$ ligands are

disposed about Ni in a distorted D_{2d} tetrahedron. By contrast, $Ni(Me_2DAD)_2$ is nearly planar. As with Cr, Mn and Cu, this demonstrates that the D_{2d} structure is electronically unstable with respect to Jahn-Teller distortion, but that this can be frustrated by steric hindrance depending on the choice of alkyl group. Metal-ligand bonding in the complexes with less bulky ligands is therefore substantially stronger. Such strain energy due to bulky ligands can therefore be released when ligands are lost, *e.g.* during CVD/ALD reactions at surfaces.

Cu(DAD)₂: As can be seen in Figure 1, fewer spin states are available for copper than for the other transition metals considered here. Coupling between doublet $Cu(II):3d^9$ ($S_M=1/2$) and triplet DAD^- ligands ($S_L=1$) can be ferromagnetic ($S_{tot}=3/2$) or partially-antiferromagnetic ($S_{tot}=1/2$). The same spin states would exist for a hypothetical Sc(II) diazadienyl complex. For Cu, a low-spin BS state is computed to be lowest in energy and the energy of the spin-pure $S_{tot}=1/2$ state is thus estimated. Analysis of the BS spin density confirms that remnant spin is located on the ligands. The lack of complete antiferromagnetic coupling evidently destabilises the complex, as no Cu complex could be isolated experimentally. This may indicate that remnant spin on ligands makes them unstable radicals. This is perhaps the background to the observation by Knisley *et al.* that the high positive reduction potential of copper cations leads to immediate reduction to the metal by the ligands.¹⁴ The computed C-C bond lengths indicate that both ligands in $Cu(^tBu_2DAD)_2$ are monoanionic. The partial absence of spin-pairing in Cu-N bonding orbitals is evident in slight lengthening of Cu-N in the BS state relative to the high-spin state. Jahn-Teller distortion towards planar Cu(II) is frustrated by substituents on N, with a strain energy of 20-50 kJ/mol depending on spin state.

Looking at the trends in electronic structure across the transition metals, we predict that **Zn(^tBu₂DAD)₂** would be qualitatively similar to $Cu(^tBu_2DAD)_2$: an unstable triplet complex with remnant spin on the ligands due to the lack of unpaired d electrons for antiferromagnetic coupling. As a d^{10} metal cation, there would be no tendency to Jahn-Teller distortion in the Zn complex and so it would be less strained than the Cu complex.

REFERENCES

¹ G. Kresse, J. Furthmüller, *Comput. Mater. Sci.* **6**, 15 (1996).

² P. E. Blöchl, *Phys. Rev. B* **50**, 17953 (1994).

-
- ³ Jiří Klimeš *et al.*, *J. Phys.: Condens. Matter* **22**, 022201 (2010).
- ⁴ F. Weigend, R. Ahlrichs, *Phys. Chem. Chem. Phys.* **7**, 3297 (2005).
- ⁵ TURBOMOLE version 6.1, a development of University of Karlsruhe and Forschungszentrum Karlsruhe GmbH, 1989-2007, TURBOMOLE GmbH, since 2007; available from www.turbomole.com; R. Ahlrichs, M. Bär, M. Häser, H. Horn and C. Kölmel, *Chem. Phys. Lett.* **162**, 165 (1989); O. Treutler and R. Ahlrichs, *J. Chem. Phys.* **102**, 346 (1995); F. Weigend, O. Treutler and R. Ahlrichs, *Theor. Chem. Acc.* **97**, 119 (1997).
- ⁶ J. P. Perdew, K. Burke and M. Ernzerhof, *Phys. Rev. Lett.* **77**, 3865 (1996); J. P. Perdew, M. Ernzerhof and K. Burke, *J. Chem. Phys.* **105**, 9982-9985, (1996).
- ⁷ M. v. Arnim and R. Ahlrichs, *J. Chem. Phys.* **111**, 9183 (1999).
- ⁸ A. M. Tondreau *et al.*, *Inorg. Chem.* **52**, 635 (2013).
- ⁹ L. Noodleman, C. Y. Peng, D. A. Case and J.-M. Mouesca, *Coord. Chem. Rev.* **144**, 199 (1995).
- ¹⁰ R. Caballol *et al.*, *J. Phys. Chem. A* **101**, 7860 (1997).
- ¹¹ C. van Wüllen, *J. Phys. Chem. A* **113**, 11535 (2009).
- ¹² K. Yamaguchi, S. Yamanaka, M. Nishino, Y. Takano, Y. Kitagawa, H. Nagao and Y. Yoshioka, *Theor. Chem. Acc.* **102**, 328 (1999).
- ¹³ T. Pugh *et al.*, *Inorg. Chem.* **52**, 13719 (2013).
- ¹⁴ T. J. Knisley, M. J. Saly, M. J. Heeg, J. L. Roberts and C. H. Winter, *Organomet.* **30**, 5010 (2011).